

Article

# Experimental Study on the Flexural Behavior of Alkali Activated Fly Ash Mortar Beams

Adelino V. Lopes <sup>1</sup>, Sergio M. R. Lopes <sup>2,\*</sup> and Isabel Pinto <sup>2</sup>

<sup>1</sup> Institute for Systems and Computers Engineering, Department of Civil Engineering, University of Coimbra, 3030-788 Coimbra, Portugal; avlopes@dec.uc.pt

<sup>2</sup> Centre for Mechanical Engineering, Materials and Processes, Department of Civil Engineering, University of Coimbra, 3030-788 Coimbra, Portugal; isabelmp@dec.uc.pt

\* Correspondence: sergio@dec.uc.pt

Received: 1 June 2020; Accepted: 23 June 2020; Published: 25 June 2020



**Featured Application:** Fly ash is a byproduct from burning pulverized coal in the electric power industry and can be incorporated in cementitious concretes or in alkali activated concretes (AAC) with obvious environmental advantages. When part of AAC, it will be able to lead to products with glossy, black surfaces, which might be aesthetically appealing for some modern architectural solutions. A reinforced concrete structure is one type of such products. This document presents an experimental study on reinforced mortar beams, half of them made with fly ash and the other half made with Portland cement. Different aspects of the structural behavior are compared for possible applications of fly ash geopolymers in civil engineering structures.

**Abstract:** This work aims to study the possibility of using alkaline activated fly ash in structural members. The work, of an experimental nature, focuses on the evaluation of the behavior of simply supported beams under two symmetrical loads (four-point tests). For such study, 10 beams were built, of which, five using fly ash and the remaining five using traditional Portland cement. The test results are compared. Conclusions on the practical application of fly ash in structures were explained and, as mention later in this document, there is room for improvement. This is one of very few works on fly ash alkali activated structures and further studies are necessary in the future. Some aspects, such as shrinkage and deformability are presented as some of the negative points concerning the potential use of fly ash. These are two aspects that need more attention in future investigations.

**Keywords:** experimental study; analytical model; reinforced concrete; beams; fly ash alkali activated; bending

## 1. Introduction

The cement industry is under increasing pressure from public opinion due to its contribution to CO<sub>2</sub> emissions. To bring the cement sector in line with the 2015 Paris Agreement on climate change, its annual emissions will need to fall by at least 16 per cent by 2030 [1]. The awareness of the high level of CO<sub>2</sub> emissions is not new, but only recent international agreements and measures really forced the cement industry to intensify the search for new alternative production technologies and materials. A vision of the producers on this issue can be found in a report by Cembureau [2].

Obviously, non-cementitious materials must be considered as an alternative route of the entire road map to low emission construction production. Various research works on alternative materials to Ordinary Portland Concrete (OPC) have been published in the last three decades, but OPC continues to dominate the market at present. However, the target limits for CO<sub>2</sub> emissions might alter the competitive advantage of OPC and surely increases the demand for research on alternative materials.

This is the case of alkali activated concretes (AAC), which show some positive points concerning the strength values, durability, or environmental impacts [3].

In fact, many works have been published on AAC in the last 2–3 decades. Almost all of them have focused on the development of the material itself, including the mechanical properties. Very few studies were concerned with the structures so far. Since the size of specimens for structural studies is bigger when compared to that of specimens for mechanical properties of the material, some difficulties arise when passing from the material to structural research. Even a recent study [4] has pointed out that there are some studies in mortars, but the need for studies in concretes still persists. This means that the step from mortar to concrete is still not entirely covered and the next step from material specimens to concrete structures is also of great necessity.

From different types of AAC, alkali activated fly ash concrete has its own particularities that need to be known. One of the most important is the workability, which is directly linked with the practical application of the material in structures. Not going deeply into the topic, it should be known that the rheological behavior observed in fly ash is different from that of OPC. The commercial admixtures for improving the workability of OPC do not have similar effects in fly ash. Further explanations on this topic are available in bibliography [5].

Shrinkage is also a characteristic of fly ash concretes, which has deserved some attention. It is known that curing conditions and the liquid-to-ash ratio are very important for shrinkage, with some researchers recommending curing temperatures of around 60–70 °C (Degrees Celsius) for minimizing shrinkage [6–8]. Indeed, the few experimental studies on reinforced beams made with fly ash activated concrete found in literature followed this recommendation [9–12]. Curing conditions at this temperature level are not practical for on-site applications. Some recent studies have concentrated on curing in ambient temperatures [13–15].

Curing at specific temperatures has other effects beyond shrinkage, for instance, on strength. Therefore, it should be considered as a strong option when possible, for instance, in precast plants. However, in the opinion of the authors, the on-site practical construction at ambient temperature must not be ruled out since it is a potential application of this material. The studied reported here was trying to evaluate the possibility of application on reinforced concrete members cast on-site at ambient temperature.

As explained before, the general possibility of replacing the Portland cement with alkaline activated binders, known as geopolymers, should be considered as a strong option given the increased concerns on environmental issues. Fly ash is one of the materials that can be used in alkaline activated products. The authors have tested other materials [16], but the current document reports a study on the behavior of fly ash in structures, particularly in beams under bending. It is interesting, in particular, to evaluate the behavior of these beams under bending action, for different levels of the loading, and to compare it with that of beams built with traditional Portland cement. It should be kept in mind that the behavior in service conditions is also gaining great importance in current regulations, when compared to typical ultimate strength.

To achieve this goal, an experimental procedure was carried out, in which two groups of five beams each were built. From group to group, the beams vary in material, with five built with Portland cement binder and five with fly ash based binder. Within each group of beams, only the ratio of the reinforcement was varied in order to cover an intentional range to cover specific situations explained later. The dimensions are the same for all beams, which are about half the dimensions usually used in the laboratory and in construction.

In addition to this objective, it would be also important to theoretically estimate the behavior of beams built with new materials. A good fitting of the numerical methodologies to the behavior of such new materials needs to be verified [17].

In this work, beams with reduced dimensions were used compared to those usually used in construction. Nevertheless, they are significantly bigger than the geopolymeric specimens generally presented in the bibliography for the study of the material. It is, therefore, important not to ignore the

possible scale effects. Some studies indicate that up to a scale of 1 to 3, the differences are negligible [18]. However other studies indicated that some differences in behavior could be important, especially for large size structures [19]. Kim et al. [20] presented a study with reinforced concrete specimens, using a scale of 1:5, where it was concluded that the models present equivalent results when compared to the normal size members. However, other studies indicate some differences. Since both types of beams of this investigation, fly ash and cement, were built with equal dimensions, it would be expected that the size effects, if any, would have similar consequences. Therefore, the comparison of the results can be accepted for beams of these dimensions.

## 2. Experimental Procedure

### 2.1. Design

In the construction of the beams, the following dimensions were chosen: length  $L = 1500$  mm, width  $b = 100$  mm, and height  $h = 150$  mm. For the longitudinal reinforcing bars,  $\phi 6$  (6 mm) and  $\phi 8$  sizes were assumed with a 10 mm cover. Transversal  $\phi 4$  stirrups were used (a reinforcement factory accepted to supply this special size). Taking into account the reduced covering, it was decided to use sand (maximum particle size of  $D_{max} \leq 2$  mm) without coarse aggregates. It was intended that the reinforcement to be used, as well as the covering, would also be reduced in the same proportionality as the external dimensions of the beams.

Taking into account the objectives of the test to be carried out, it was intended that the combination of the materials allowed to obtain approximately half of the beams reaching failures by the reinforcement, and the other half by crushing of the mortar. Keeping this in mind, for the five beams to be constructed with each material, the only parameter to be varied, as uniformly as possible, would be the percentage of the reinforcement, which should cover a range of usual values in construction. That is, in addition to the dimensions, the compressed longitudinal reinforcement, the transversal reinforcement and the material in each group of beams remained constant. Obviously, the failure of the middle beam of each group could occur either by the reinforced bars or by crushing of mortar. Table 1 shows the designations adopted for the beams. In this table,  $\phi$  indicates the number and diameter of the tensioned reinforcement of the beam,  $A_s$  the corresponding area, and  $\rho$  the percentage of tensioned reinforcement.

Table 1. Designation of the beams.

| Binder     | Longitudinal Reinforcing Bars |                          |            | Label                      |                           |
|------------|-------------------------------|--------------------------|------------|----------------------------|---------------------------|
|            | $\phi$ [mm]                   | $A_s$ [mm <sup>2</sup> ] | $\rho$ [%] |                            |                           |
| Cement     | 2 $\phi$ 6                    | 56.5                     | 0.38       | Insufficiently reinforced  | Cem-2F6                   |
|            | 3 $\phi$ 6                    | 84.8                     | 0.57       | Lightly reinforced         | Cem-3F6                   |
|            | 4 $\phi$ 6                    | 113                      | 0.75       | Bellow normally reinforced | Cem-4F6                   |
|            | 3 $\phi$ 8                    | 151                      | 1.01       | Normally reinforced        | Cem-3F8                   |
|            | 4 $\phi$ 8                    | 201                      | 1.34       | Above normally reinforced  | Cem-4F8                   |
|            | Fly Ash                       | 2 $\phi$ 6               | 56.5       | 0.38                       | Insufficiently reinforced |
| 3 $\phi$ 6 |                               | 84.8                     | 0.57       | Lightly reinforced         | FA-3F6                    |
| 4 $\phi$ 6 |                               | 113                      | 0.75       | Bellow normally reinforced | FA-4F6                    |
| 3 $\phi$ 8 |                               | 151                      | 1.01       | Normally reinforced        | FA-3F8                    |
| 4 $\phi$ 8 |                               | 201                      | 1.34       | Above normally reinforced  | FA-4F8                    |

One of the initial concerns was to obtain failure by bending and not by shear. Since the critical beam would be the one under the greatest loads, it was decided to fix an amount of stirrups, which would prevent shear failure for such beam, and to use the same amount of transverse reinforcement in all the beams. Following this option, identical conditions of material confinement in all beams would also be guaranteed. This parameter is very important in bending beams. This led to 4 mm diameter

transverse reinforcement bars ( $\phi 4$ ) made by two branches stirrups spaced 70 mm. In the top of the beam, 2  $\phi 6$  longitudinal bars were used. Figure 1 shows the reinforcement before casting.



**Figure 1.** Beams before casting.

## 2.2. Materials

Apart from the especial size 4 mm bars, which were courtesy of a factory nearby [21], the rest of the reinforcing bars were bought in the market. All of the bars were tested according to standard NP EN 10002-1 [22]. In these tests, four samples of each type of steel, about 40 cm long, were used. Table 2 shows the averages values of yield strength of reinforcement ( $f_{sy}$ ), ultimate strength of reinforcement ( $f_{su}$ ), and strain of reinforcement steel at maximum load ( $\epsilon_{su}$ ).

**Table 2.** Mechanical characteristics of steel bars.

| Diameter [mm] | $f_{sy}$ [MPa] | $f_{su}$ [MPa] | $f_{su}/f_{sy}$ | $\epsilon_{su}$ [%] |
|---------------|----------------|----------------|-----------------|---------------------|
| 4             | 524            | 665            | 1.27            | 5.0                 |
| 6             | 572            | 823            | 1.44            | 5.0                 |
| 8             | 614            | 706            | 1.15            | 11.1                |

The granulometry of the coarse aggregates to be used in the mixtures was conditioned by the size of the specimens to be cast, especially the cover. It was found that the size of the aggregates would not be appropriate and they were not used. A sand was used.

For the mortar production, Normal Portland Type I CEM I 42.5 R cement (Compressive Strength = 42.5 MPa) was used, from CIMPOR. According to the producing company, this material consists essentially of CaO (61.5%) and SiO<sub>2</sub> (21%).

The fly ash came from the Sines thermal power plant and resulted from the burning of coal. The ashes are certified by the National Laboratory of Civil Engineering (LNEC); thus, fulfilling the compliance and performance requirements defined in Annex ZA of standard NP EN450-1 [23]. Its composition essentially contains calcium oxide, CaO (71%) and potassium oxide, K<sub>2</sub>O (16%), according to tests carried out at the Department of Earth Sciences of the University of Coimbra. Moreover, for these ashes, the high specific surface leads to great reactivity. An activator needs to be used; it must be dosed and concentrated by taking into account the binder, namely its chemical composition, and the degree of fineness that influence the activation reaction. In this work, it was decided to use an activator composed of sodium hydroxide (NaOH) and sodium silicate (NaSiO<sub>3</sub>), in the proportion of 1:2, respectively. The NaOH was obtained by mixing caustic soda with water in the appropriate proportions so that the 12.5 M molal concentration of NaOH could be achieved following the indications given by Pinto [24]. This decision also took into account the experience of other works carried out at the host laboratory regarding workability, and also the limits of the molar

concentration of NaOH so that the alkaline reaction occurs in full: 12 M according to Granizo [25] and 20 M according to Davidovits [26]. The second component of the activator, sodium silicate (“D40”) was purchased from the company “Quimitecnica”.

### 2.3. Production of Beams

The cement mortar was produced at Department of Civil Engineering of the University of Coimbra, as well as the tests carried out on small specimens (cubes and prisms) and on the beams. To follow the initial objectives, an average strength of 35 MPa was targeted for the beams. For this purpose, a mixture was carried out. The mix proportions were 270 kg of sand, 60 kg of cement, 30 kg of water, and 0.54 kg of superplasticizer Sika ViscoCrete 20HE. This mixture was sufficient for casting five beams, twelve 150 mm cubes, and six 40 × 40 × 160 mm prisms. After three days of curing, the beams, cubes and prisms were demolded.

The fly ash based mixture was done with: 200 kg of sand, 80 kg of fly ash, and 40 kg of compound activator. These proportions were those adopted from a base recipe suggested by Pinto [27]. With this mixture, five beams, twelve 40 × 40 × 160 mm prisms, and five 150 mm cubes were cast and demolded five days later.

Table 3 shows the weight and real dimensions, measured after the construction of the beams. The height (h) and the width (b) result from an average of three measurements made in the central area of the beam (the most important area of the tests). L represents the length of the beam. It appears that the greatest deviations occurred for the height (h).

**Table 3.** Effective dimensions of the beams.

| Beam    | Weight [kg] | b [mm] | h [mm] | L [mm] |
|---------|-------------|--------|--------|--------|
| Cem-2F6 | 52.1        | 98.1   | 152    | 149.5  |
| Cem-3F6 | 53.9        | 100    | 153    | 149.5  |
| Cem-4F6 | 54.9        | 100    | 154    | 149.5  |
| Cem-3F8 | 54.6        | 101    | 153    | 149.5  |
| Cem-4F8 | 53.4        | 97.4   | 152    | 149.5  |
| FA-2F6  | 51.9        | 104    | 152    | 149.6  |
| FA-3F6  | 51.7        | 99.3   | 152    | 149.6  |
| FA-4F6  | 52.2        | 99.2   | 153    | 149.5  |
| FA-3F8  | 52.7        | 102    | 153    | 149.5  |
| FA-4F8  | 53.2        | 103    | 152    | 149.5  |

Control tests were carried out on cubes and prisms, on different days, in order to evaluate the evolution of the strength.

Regarding the cement mortar tests, the results on cubes gave very close results to the expected average compressive strength of the concrete, an exponential curve proposed by Neville [28] (see Figure 2). In this figure,  $f_{cm}$  indicates the average value of the compressive strength of concrete for the time T in days.

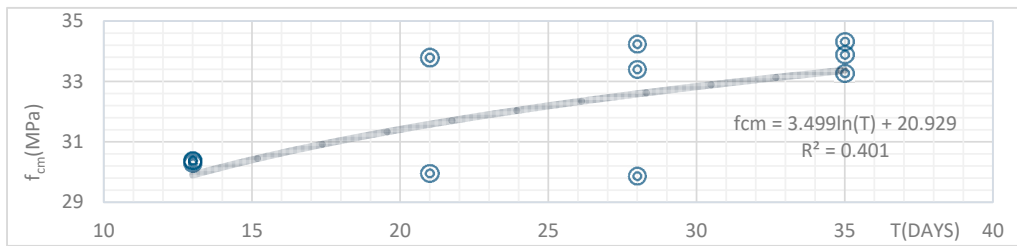


Figure 2. Average strength of the cement specimens.

Regarding the fly ash specimens, compression and/or tension strength tests were performed on twelve 40 × 40 × 160 mm test specimens, following NP EN 196-1 and NP EN12390-5 [29,30], to determine the mechanical characteristics of this material. The value for the modulus of elasticity of this material was about 20 GPa in non-destructive cyclic tests and about 18 GPa in failure tests. The average compressive and tensile strengths were 15.1 and 3.2 MPa at 23 days old and 23.5 and 4.0 MPa at 32 days old, respectively. The corresponding maximum stresses were respectively, 17.8 and 3.3 MPa at 23 days and 30.7 and 4.6 MPa at 32 days. From the compression tests of 150 mm cubes, an average compressive strength of 23.8 MPa, was obtained at 32 days, with a maximum value of 27.2 MPa. The standard deviation of the results was 2.6. It should be noted that all ash beams were tested between days 31 and 33 after pouring.

2.4. Test Procedure

Figure 3 shows the symmetric loading diagram adopted for the beam tests. The beams were simply supported, and the supports were placed at 50 mm from each end. Two vertical symmetrical loads P/2 were placed 450 mm apart, leading to pure flexion. A central zone of the beam was then under a constant bending moment. The self-weight was not considered in the diagrams shown in this figure.

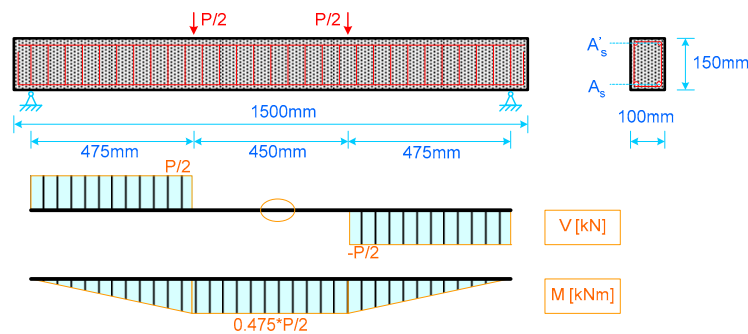


Figure 3. Load set-up and shear and bending diagrams.

A beam under test is shown in Figure 4. The evaluation of the deformation of the beams (the deflection) was carried out using nine Linear Variable Differential Transformers (LVDTs). Three of them were placed on each support (to measure vertical and horizontal displacements) and three others were placed in the central zone (to measure the mid span deflection), as shown in Figure 4.

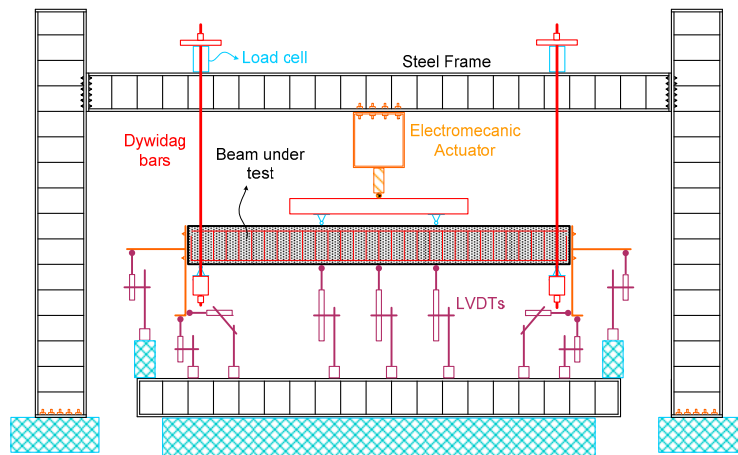


Figure 4. Beam under test.

The readings of the load cells and LVDTs were recorded by a Data Logger TML TDS-602, with a frequency of 2 Hz.

### 3. Test Results

The comparison of the behavior of the beams is based on key aspects of the evolution of the beam with load, such as the cracking point,  $P_{cr}$ , the yielding of steel,  $P_y$ , the maximum load,  $P_{max}$ , the ultimate strength,  $P_{ult}$ , among others. The stiffness in each zone of the P-d graph is also an important aspect for comparison. The P-d diagram will be the basis for this analysis (P corresponds to the total load applied at each instant, and d to the displacement in the mid-span of the beam). The load P is obtained from the sum of the loads registered in the four load cells responsible for measuring the value of the support reactions. The value of the displacement in the mid-span, d, is obtained by subtracting the value of the LVDTs at the supports from the value measured of the LVDT placed in the mid-span of the beam.

The test results are presented in Figures 5–9. This type of beams generally presents three distinct phases in behavior, namely: State I, State II, and State III. State I, which corresponds to the Stiffness  $K_I$ , extends from the origin to the point  $P_{cr}$ , corresponding to the beginning of cracking. The second state, Stiffness  $K_{II}$ , goes from  $P_{cr}$  to the point where the reinforcement yields  $P_y$ . Finally, the third and last State is the “plastic phase” and starts at  $P_y$  and extends past the maximum load  $P_{max}$ , and ending at the last load point  $P_{ult}$  ( $P_{ult}$  is assumed to be the load 15% lower than the maximum load, according to NP EN1998-1 [31]). In beams where the failure occurs due to reinforcement failure, this point generally coincides with the last point of the graph.

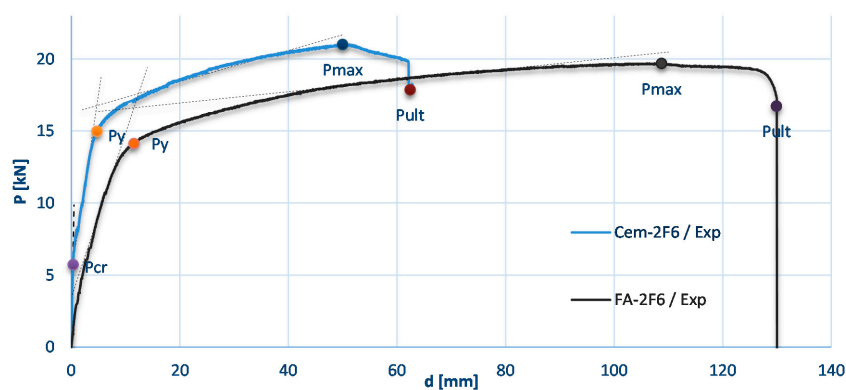


Figure 5. P-d experimental curves for beams Cem-2F6 and FA-2F6.

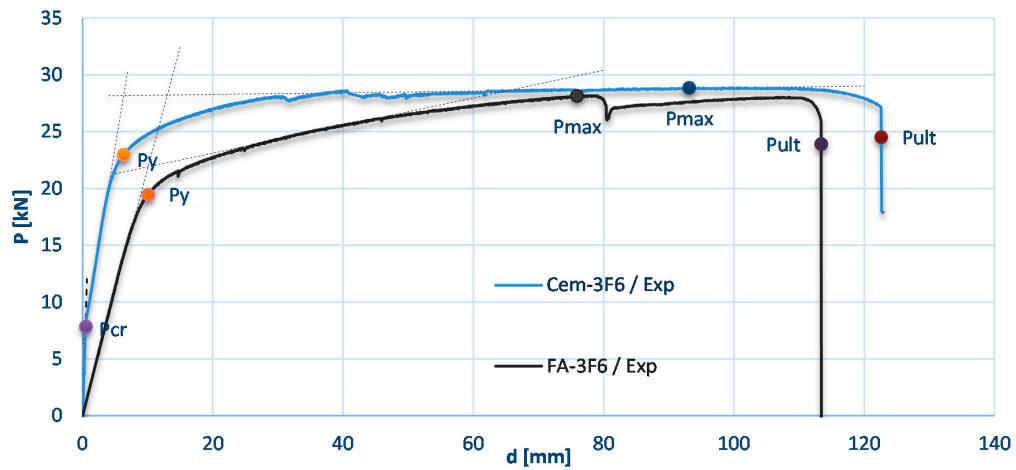


Figure 6. P-d experimental curves for beams Cem-3F6 and FA-3F6.

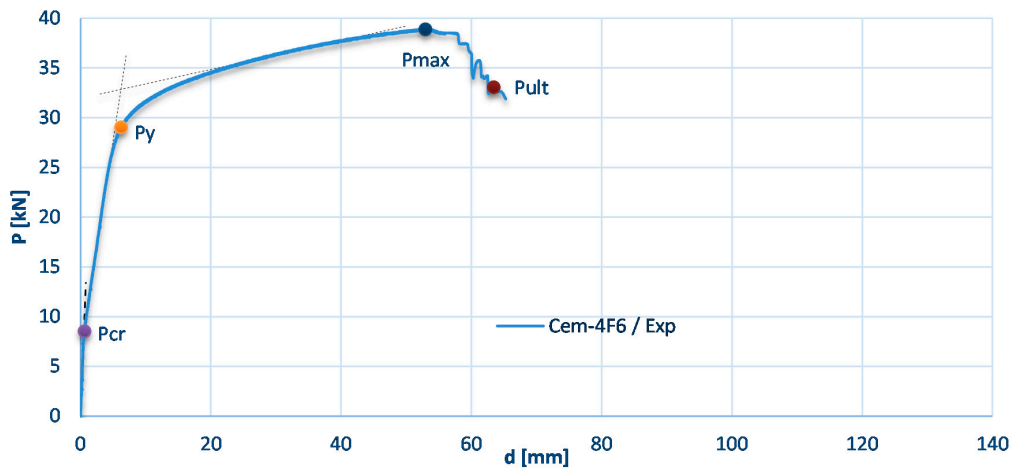


Figure 7. P-d experimental curve for beam Cem-4F6.

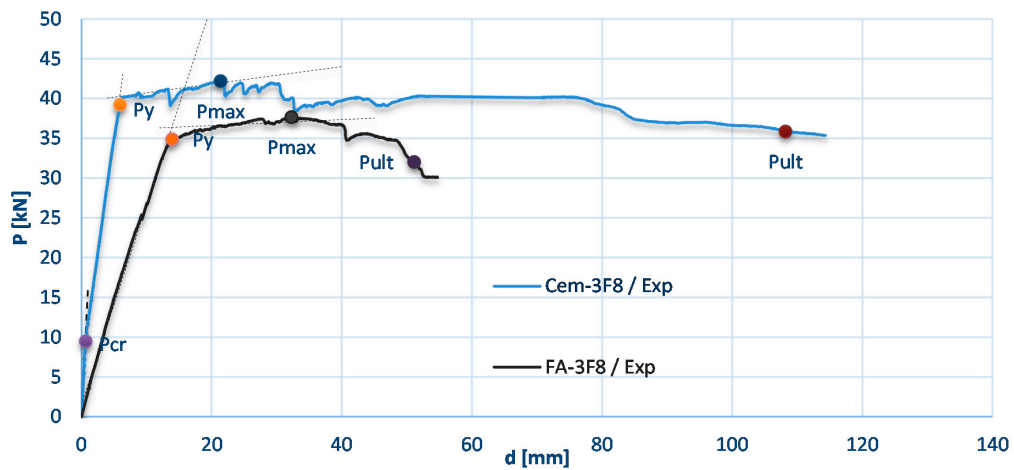


Figure 8. P-d experimental curves for beams Cem-3F8 and FA-3F8.

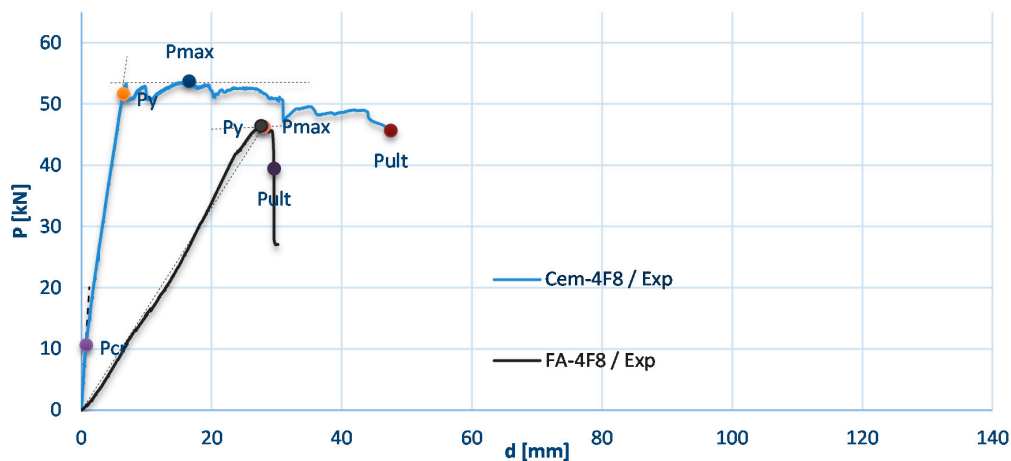


Figure 9. P-d experimental curves for beams Cem-4F8 and FA-4F8.

Figure 5 shows the P-d curves (load-deflection curves) for the insufficiently reinforced beams ( $\rho = 0.38\%$ ). The absence of State I in the fly ash beam curve is justified by the fact that these beams were cracked before the start of the test. This was provoked by the shrinkage due to the temperature of the curing time. This outcome was an assumed risk and could not be ruled out before casting. Since it did occur, this is an issue that needs to be further investigated. To cast these fly ash structures only under an optimized curing temperature of 60 to 70 degrees centigrade seems to be too restrictive to practical construction on site. Apart from this, it appears that there are no significant differences between both types of beams in terms of the stiffness of State II, nor in the values of  $P_y$  and  $P_{max}$  loads. In this case, the fly ash beam proved to be much more flexible and more ductile when compared to Cement (Cem) beam.

Figure 6 shows the P-d curves of the lightly reinforced beams ( $\rho = 0.57\%$ ). In State II, both types of beams have similar behavior. In terms of ductility, the beams are equivalent, showing both a long level of ductility, despite the type of steel used for reinforcement (cold hardened steel).

Figure 7 shows the P-d curve for beam CEM-4F6 (below normally reinforced:  $\rho = 0.75$ ). Unfortunately, a rare malfunction of the data logger caused the loss of the recorded values of FA-4F6 beam. The relatively low value of the ductility of the beam stands out in this experimental curve.

Figure 8 shows the P-d diagrams of the normally reinforced beams ( $\rho = 1.01\%$ ). Looking at the  $P_y$  and  $P_{max}$  points, it is clear that the ductility of the cement beams is much higher than that of the fly ash beam.

Figure 9 shows the P-d curve of above normally reinforced beams ( $\rho = 1.34\%$ ). In this case, the ash beam revealed an absence of ductility. The cement beams also show a low level of ductility, which could be problematic for hyperstatic structures under seismic actions, for instance. The values of  $P_y$  and  $P_{max}$  are not very different when both beams are compared. However, the modulus of elasticity in State II is noticeably smaller for the fly ash beam when compared to cement beam. This means that the first beam is more flexible than the second one.

Table 4 shows some further information related to the tests. The “curing” refers to the age of the beam in the day of testing,  $\Delta T$  is the duration of the test, and “failure by” means the type of failure shown in the tests, whether by the tensioned reinforcement, “As”, by crushing the compressed material, “fc”, or by failure of the stirrups, “V”. Thus, all beams were tested in the time ranging from 31 to 37 days. In the case of insufficiently reinforced or lightly reinforced beams, the failure occurred due to the failure of the tensioned reinforcement, as expected. In the other cases, the failures occurred due to crushing of the compressed material, except for the FA-3F8 beam, where the failure occurred in a shear crack, in this case due to insufficient connection of the stirrup to the surrounding material (this was observed during the visual inspection of the zone after the test).

**Table 4.** Further information related with tests.

| Beam             | 2F6 |     | 3F6 |     | 4F6 |     | 3F8 |     | 3F8 |    |
|------------------|-----|-----|-----|-----|-----|-----|-----|-----|-----|----|
|                  | Cem | FA  | Cem | FA  | Cem | FA  | Cem | FA  | Cem | FA |
| Curing [days]    | 34  | 32  | 34  | 32  | 36  | 32  | 37  | 31  | 35  | 31 |
| $\Delta T$ (min) | 230 | 191 | 146 | 142 | 370 | 147 | 193 | 102 | 219 | 83 |
| Failure by:      | As  | As  | As  | As  | fc  | fc  | fc  | fc  | fc  | V  |

$\Delta T$  = duration of test; As = failure by longitudinal steel bars; fc = failure by crushing of concrete; V—failure by shear (stirrups).

Table 5 shows the values obtained from the curves of the tested beams. Some conclusions are obvious. For example, yield and maximum loads increase as the maximum pulling force on steel increases (due to higher values of the area of cross section of the sum of the longitudinal bars). However, there are some other important trends in this table. For example, although there are no significant variations in the rigidity of State I, at point  $P_{cr}$ , the crack load increases significantly with As, as it was theoretically demonstrated in a previous publication [32].

**Table 5.** Parameters associated with the behavior of the beams.

| Beam              | 2F6  |      | 3F6  |      | 4F6  |       | 3F8  |      | 3F8  |      |
|-------------------|------|------|------|------|------|-------|------|------|------|------|
|                   | Cem  | FA   | Cem  | FA   | Cem  | FA    | Cem  | FA   | Cem  | FA   |
| $P_{cr}$ [kN]     | 5.73 | –    | 7.87 | –    | 8.55 | –     | 9.47 | –    | 10.6 | –    |
| $d_{cr}$ [mm]     | 0.34 | –    | 0.49 | –    | 0.60 | –     | 0.59 | –    | 0.73 | –    |
| $K_I$ [kN/mm]     | 19.7 | –    | 17.2 | –    | 16.7 | –     | 15.9 | –    | 16.8 | –    |
| $P_y$ [kN]        | 15.0 | 13.8 | 23   | 19.2 | 29.0 | –     | 39.2 | 34.9 | 51.6 | 45.5 |
| $d_y$ [mm]        | 4.70 | 12.1 | 6.29 | 9.54 | 6.21 | –     | 5.68 | 15.3 | 6.42 | 24.3 |
| $K_{II}$ [kN/mm]  | 2.50 | 1.36 | 3.48 | 2.25 | 4.27 | –     | 5.86 | 2.37 | 7.41 | 1.91 |
| $P_y/P_{cr}$      | 2.61 | –    | 2.92 | –    | 3.40 | –     | 4.14 | –    | 4.86 | –    |
| $K_I/K_{II}$      | 7.87 | –    | 4.93 | –    | 3.83 | –     | 2.7  | –    | 2.26 | –    |
| $P_{max}$ [kN]    | 21.0 | 19.7 | 28.8 | 21.5 | 38.9 | ~33.0 | 42.2 | 37.7 | 53.7 | 46.4 |
| $d_{max}$ [mm]    | 49.9 | 110  | 93.1 | 75.7 | 52.9 | –     | 21.3 | 33.6 | 16.5 | 25.4 |
| $K_{III}$ [kN/mm] | 0.11 | 0.04 | 0.01 | 0.12 | 0.15 | –     | 0.11 | 0.04 | 0.00 | 0.05 |
| $P_{max}/P_y$     | 1.40 | 1.43 | 1.26 | 1.12 | 1.34 | –     | 1.08 | 1.08 | 1.04 | 1.02 |
| $d_{ult}$ [mm]    | 62.4 | 131  | 123  | 113  | 63.4 | ~81   | 108  | 52.4 | 47.5 | 27.4 |
| $d_{ult}/d_y$     | 13.3 | 10.9 | 19.5 | 11.9 | 10.2 | –     | 19.0 | 3.43 | 7.41 | 1.13 |

Another important aspect is the general idea that the ductility of a structure is related to the ductility of the steel bars. Assuming the  $d_{ult}/d_y$  as an indicator of the ductility of a beam, it appears that a high ductility of the beams could occur with low ductility steel, as that used in this experimental program. As explained before [33,34], ductility depends on other concrete confinement conditions, which could be much more important.

Another important aspect concerns the  $K_I/K_{II}$  quotient. Eurocode 2, EC2 [35] proposes a value of 3 for this quotient. According to the results obtained for these five cement beams, this quotient can be related to the percentage of reinforcement,  $\rho$ , or to the mechanical percentage of reinforcement,  $\omega$ , through equations 1. The equations result from an adjustment of the results to an exponential curve ( $R^2 = 0.98$ ).

As previously mentioned, the ash beams did not show State I (not cracked). In addition, the deformability was generally higher than that of the cement beams (due to lower  $K_{II}$  stiffness values). The ductility of the fly ash beams was always lower than that of the cement beams.

$$\frac{K_I}{K_{II}} = 0.0292\rho^{0.995}; \frac{K_I}{K_{II}} = 0.495\omega^{0.914} \quad (1)$$

Table 6 shows the deviations of the values of the fly ash beams in relation to those of the cement beams. In this study, it is important to start by mentioning that the value of the compressive strength of the fly ash (~23.5 MPa; 23.8 MPa in cubes) is much lower (−29%) than that found for the cement specimens (~33 MPa). In any case, the loads at the  $P_y$  points are about 10 to 15% lower. The behavior tends to be more similar for  $P_{max}$ .

**Table 6.** Deviations from the key values of the strength of the beams.

| Viga              | 2F6          | 3F6          | 3F8          | 4F8          |
|-------------------|--------------|--------------|--------------|--------------|
|                   | (Cem-FA)/Cem | (Cem-FA)/Cem | (Cem-FA)/Cem | (Cem-FA)/Cem |
| $P_y$ [kN]        | −8.0%        | −17%         | −11%         | −12%         |
| $d_y$ [mm]        | 157%         | 52%          | 169%         | 279%         |
| $K_{II}$ [kN/mm]  | −46%         | −35%         | −60%         | −74%         |
| $P_{max}$ [kN]    | −6.2%        | −25.3%       | −11%         | −14%         |
| $d_{max}$ [mm]    | 120%         | −19%         | 58%          | 54%          |
| $P_{max}/P_y$ [1] | 2.1%         | −11%         | 0%           | −2%          |
| $d_{ult}$ [mm]    | 110%         | −8%          | −51%         | −42%         |
| $d_{ult}/d_y$     | −18%         | −39%         | −82%         | −85%         |

The great difference between the behavior of ash beams when compared to that of the cement beams lies in the flexibility throughout State II. As a consequence, deformations at the  $P_y$  point are the ones with the greatest deviations. However, deformations at the  $P_{ult}$  point are lower for ash beams, which indicates lower ductility of ash beams when compared to that of the cement beams.

#### 4. Theoretical Analysis

To complete this study, the authors have decided to use a nonlinear analysis algorithm [17,33,34,36] that they have already applied in other reinforced concrete (RC) beams before. For applying to the beams of the current investigation, as the input of the numerical procedure the experimental stress-strain curves of the materials were considered, both for the steel and for the mortar materials. However, the key parameters values of each stress-strain curve were deduced also by using the information of the tests of the beams.

For the fly ash beams, the tension part was not considered because the beams were cracked before tests, as explained before. However, the predicted behavior of un-cracked fly ash beams was also computed for added information.

Figures 10–14 show the curves for the 5 sets of beams. In these figures, the experimental curves are in continuous line and the theoretical curves are dashed. The red color represents the curves for the cement beams, and the grey color the curves for the fly ash beams. The blue dashed line (theoretical 2) represents the curve for the ash beams, in case the retraction problem could be minimized (beams with no cracks before testing).

These figures show a very good approximation of the theoretical curves to the experimental ones for the cement beams. The least successful approach occurred for beam Cem-3F6. Despite the attention put in these simulations it is not possible to simulate some deficiencies not detected in the beams, or some details that favor their strength.

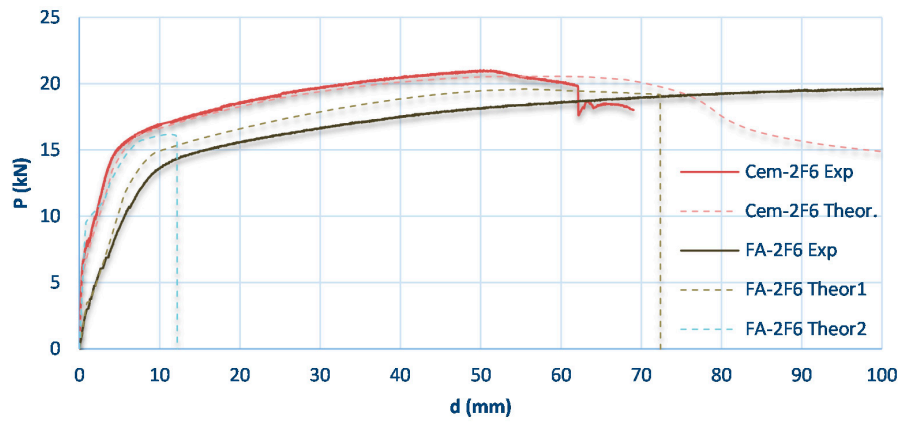


Figure 10. P-d curves for beams Cem-2F6 and FA-2F6.

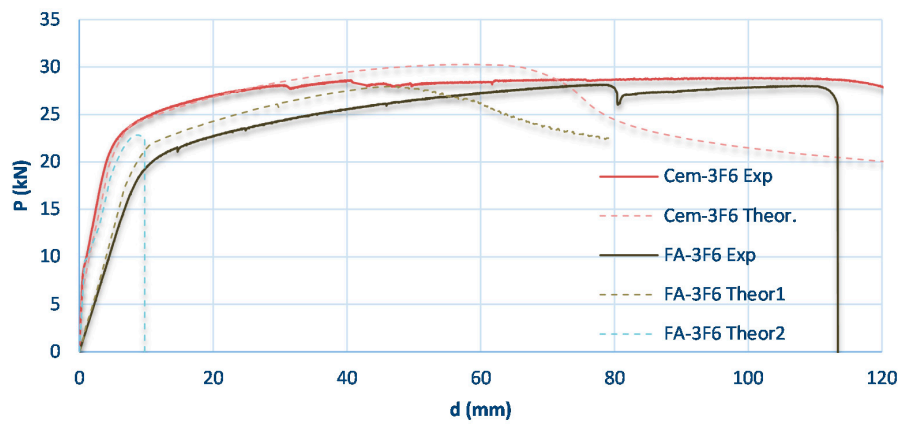


Figure 11. P-d curves for beams Cem-3F6 e FA-3F6.

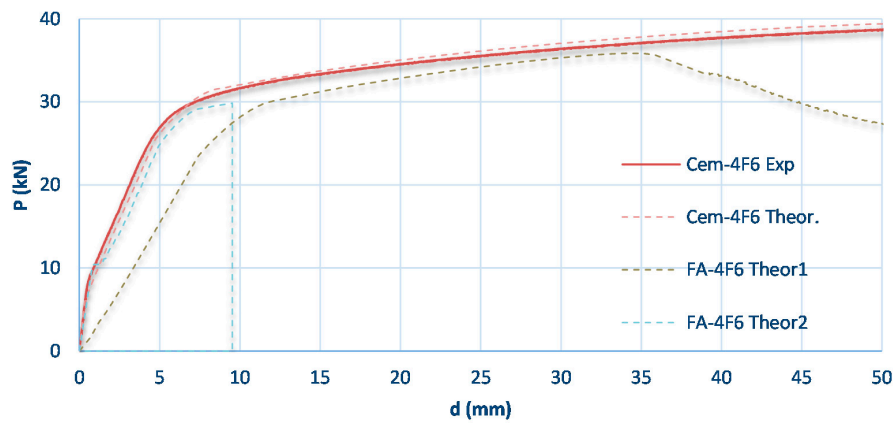


Figure 12. P-d curves for beams Cem-4F6 e FA-4F6.

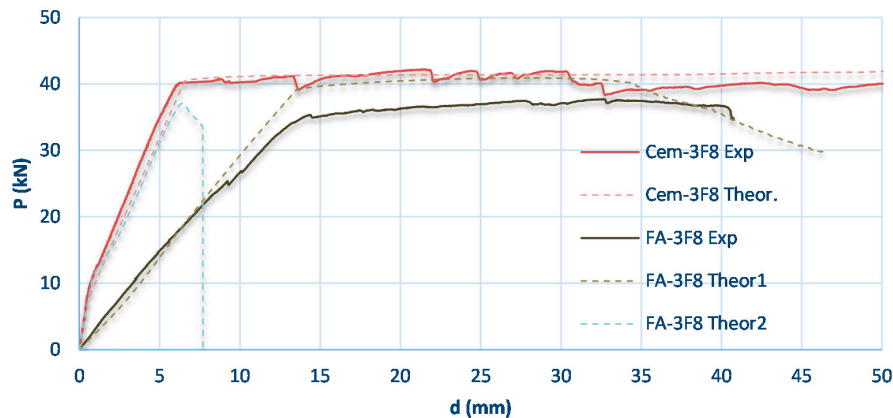


Figure 13. P-d curves for beams Cem-2F8 e FA-2F8.

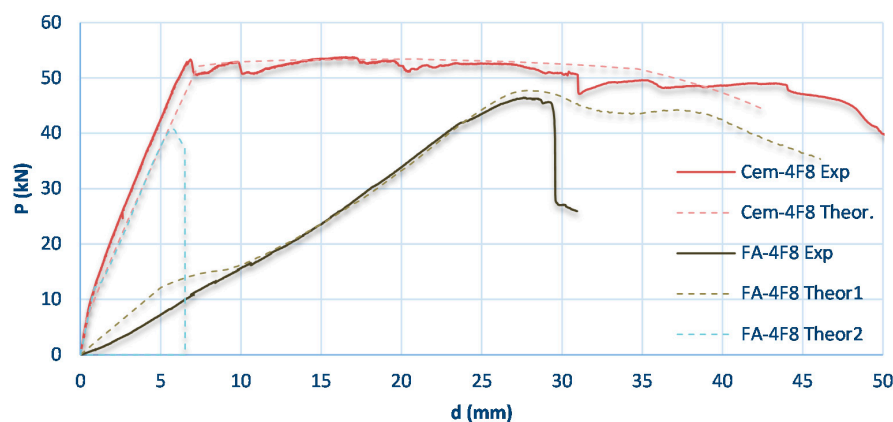


Figure 14. P-d curves for beams Cem-3F8 e FA-3F8.

In the case of fly ash beams, the discrepancies between the theoretical curves and the experimental curves are more significant. Assuming that the behavior of the steel bars is correct (the reinforcing bars of cement beams were the same as those of fly ash beams), these discrepancies can only be originated from the variability of the mortar material (fly ash), which in fact was confirmed in the laboratory. Beam FA-4F8 was the one that showed the highest degree of initial cracking.

In Figure 12, for beam 4F6, there is no experimental curve for the ash beam, as previously mentioned. However, the experimental curves can be presented on the assumption that the fly ash material was similar to the remaining fly ash beams.

The curves called “Theor. 2” corresponded to the behavior of the beams if the behavior of the material was the one verified in the tests of the  $40 \times 40 \times 160$  mm prisms, and of the cubes, namely in terms of compressive strength, tensile strength, and modulus of elasticity (as mentioned before, the beams were already cracked before testing). There are important aspects to this prediction. Firstly, for low levels of loading, the curves of the fly ash beams are close to those of the cement beams. In a second aspect, it appears that the beams show lower maximum loads. However, the worse aspect of their behavior when compared to the cement beams, is a very low ductility, since their ultimate load (85%  $P_{max}$ ) occurs for very small deformations ( $L/d_{ult} \sim 140$ ). For comparison, all the cement beams were at least 5 times more ductile.

## 5. Conclusions

As previously stated, the number of studies on beams made from fly ash geopolymers are very scarce. This was probably the first study with curing at ambient temperature. The (very few) past experimental studies on beams of this material were carried out using special equipment to cure the material at 60 to 70 °C, which is rather difficult to implement outside a laboratory or a precast plant.

The risk of effects due to shrinkage was real, but it was not visible in small specimens, such as prisms or cubes. In the larger masses, such as the test beams, probably due to the presence of the reinforcing bars, the internal constraints led to some cracking during the hardening of the beams. Possibly, with other types of reinforcing, such as Fiber Reinforced Plastics, FRPs, this problem could be avoided, depending on the modulus of elasticity of such material.

In addition, three other aspects were found to be important in fly ash geopolymers beams when compared to cement beams: The low modulus of elasticity, the relatively low value of the maximum compressive strength, and the reduced values of the ductility.

Regarding the low modulus of elasticity of the fly ash beams, it does not prevent this material from being used in structures. Regarding the reduced value of the maximum compressive stress, this has natural influence on the ultimate and service loads. Cross sections need to be bigger than those of cement beams and this makes the inertia higher and, consequently, this can compensate the low modulus of elasticity when deformations have to be limited to certain values ( $L/400$ , for instance).

The reduced deformation after the peak load penalizes the ductility of this type of beams. This could be problematic when ductility is important, such as in seismic zones or in hyperstatic structures when redistribution of moments is expected.

In general, this material still needs further developments in order to reduce shrinkage for castings at ambient temperature and to increase the compressive strength. A potential use might be in railway sleepers for instance.

**Author Contributions:** All authors were involved in all parts of the work, but with different weights, as described next. For Conceptualization, methodology, analysis and writing: A.V.L., S.M.R.L., and I.P.; experimental work: A.V.L. and I.P.; computing of data: A.V.L.; final editing: S.M.R.L. All authors have read and agreed to the published version of the manuscript.

**Funding:** This research was sponsored by FEDER funds through the program COMPETE—Programa Operacional Factores de Competitividade—and by national funds through FCT—Fundação para a Ciência e a Tecnologia—, under the project UIDB/00285/2020.

**Acknowledgments:** The authors would like to express their gratitude to L.C. of the Department of Earth Sciences of the University of Coimbra and to A.T.-P. of the Technical Institute of Tundavala for the collaboration in this study. They also want to thank EDP—G.d.P.d.E. S.A., represented by H.F., for the donation of fly ashes and FAPRICELA, S.A., represented by N.B., for the donation of steel bars. Finally, they want to express their gratitude to the students N.M.d.S.C., A.S.G., and J.A.S.R., who have also collaborated in this investigation.

**Conflicts of Interest:** The authors declare no conflict of interest.

## References

1. Lenne, J.; Preston, P. *Making Concrete Change—Innovation in Low-Carbon Cement and Concrete*; Chatham House, the Royal Institute of International Affairs: London, UK, 2018; p. 138.
2. Cembureau. *The Role of Cement in the 2050 Low Carbon Economy*; Cembureau: Brussels, Belgium, 2013; p. 64.
3. Teixeira-Pinto, A. *Sistemas Ligantes Obtidos por Activacao Alcalina do Metacaulino (Binder Systems Obtained by Alkaline Activation of Metakaolin)*. Ph.D. Thesis, University of Minho, Guimaraes, Portugal, 2004. (In Portuguese).
4. Ling, Y. *Proportion and Performance Evaluation of Fly Ash-Based Geopolymer and its Application in Engineered Composites*. Ph.D. Thesis, Iowa State University, Ames, IA, USA, 2018; p. 151.
5. Criado, M.; Palomo, A.; Fernandez-Jimenez, A.M.; Banfill, P.F.G. Alkali activated fly ash: The effect of admixtures on paste rheology. *Rheol. Acta* **2009**, *48*, 447–455. [[CrossRef](#)]
6. Riddirud, C.; Chindaprasirt, P.; Pimraksa, K. Factors affecting the shrinkage of fly ash geopolymers. *Int. J. Miner. Metall. Mater.* **2011**, *18*, 100–104. [[CrossRef](#)]
7. Vijayakumar, R.M. *Evaluating Shrinkage of Fly Ash—Slag Geopolymers*. Master's Thesis, University of Illinois at Urbana-Champaign, Champaign, IL, USA, 2013; p. 55.
8. Wattimena, O.K.; Antoni; Hardjito, D. A review on the effect of fly ash characteristics and their variations on the synthesis of fly ash based geopolymer. In *Green Construction and Engineering Education for Sustainable Future AIP Conference Proceedings*; Petra Christian University: Kota SBY, Indonesia, 2017; pp. 020041:1–020041:12.

9. Abraham, R.; Raj, S.D.; Abraham, V. Strength and behaviour of geopolymer concrete beams. In Proceedings of the International Conference on Energy and Environment-2013 (ICEE 2013), Putrajaya, Malaysia, 5–6 March 2013; pp. 158–163.
10. Kumaravel, S.; Thirugnanasambandam, S. Flexural behaviour of geopolymer concrete beams. *Int. J. Adv. Engg. Res. Stud. III I* **2013**, *6*, 1–4.
11. Monfardini, L.; Minelli, F. Experimental study on full-scale beams made by reinforced alkali activated concrete undergoing flexure. *Materials* **2016**, *9*, 739. [[CrossRef](#)] [[PubMed](#)]
12. Ahmed, H.Q.; Jaf, D.K.; Yaseen, S.A. Comparison of the flexural performance and behaviour of fly-ash-based geopolymer concrete beams reinforced with CFRP and GFRP bars. *Adv. Mater. Sci. Eng.* **2020**, *2020*, 1–15. [[CrossRef](#)]
13. Fang, G.; Bahrami, H.; Zhang, M. Mechanisms of autogenous shrinkage of alkali-activated fly ash-slag pastes cured at ambient temperature within 24 h. *Constr. Build. Mater.* **2018**, *171*, 377–387. [[CrossRef](#)]
14. Samantasinghar, S.; Singh, S.P. Fresh and hardened properties of fly ash-slag blended geopolymer paste and mortar. *Int. J. Concr. Struct. Mater.* **2019**, *13*, 47. [[CrossRef](#)]
15. Biondi, L.; Perry, M.; Vlachakis, C.; Wu, Z.; Hamilton, A.; McAlorum, J. Ambient cured fly ash geopolymer coatings for concrete. *Materials* **2019**, *12*, 923. [[CrossRef](#)] [[PubMed](#)]
16. Lopes, A.V.; Lopes, S.M.R.; Pinto, M.I.M. Influence of the composition of the activator on mechanical characteristics of a geopolymer. *Appl. Sci.* **2020**, *10*, 3349. [[CrossRef](#)]
17. Lopes, A.V.; Lou, T.J.; Lopes, S.M.R. Numerical Evaluation of the Non Linear Behaviour of Reinforced Concrete Beams. In Proceedings of the 14th International Conference on Civil, Structural and Environmental Engineering Computing, Cagliari, Sardinia, Italy, 3–6 September 2013; Civil-Comp Press: Stirlingshire, UK, 2013; p. 115.
18. Kim, J.K.; Yi, S.T.; Kim, J.H.J. Effect of specimen sizes on flexural composite strength of concrete. In *Fracture Mechanics of Concrete Structures*; Borst, Ed.; Smets & Zeitlinger: Lisse, Holland, 2001; pp. 697–704.
19. Carpinteri, A.; Chiaia, B. Embrittlement and decrease of apparent strength in large-sized concrete structures. *Sadhana* **2002**, *27*, 425–448. [[CrossRef](#)]
20. Kim, N.; Lee, J.; Chang, S. Equivalent multi-phase similitude law for pseudodynamic test on small scale reinforced concrete models. *Eng. Struct.* **2009**, *31*, 834–846. [[CrossRef](#)]
21. Fapricela. Available online: <https://www.fapricela.pt/> (accessed on 27 May 2020).
22. NP EN10002-1. *Materiais Metálicos. Ensaios de Tracção—Parte 1: Método de Ensaio à Temperatura Ambiente (Tensile Testing of Metallic Materials. Method of Test at Ambient Temperature)*; Instituto Português da Qualidade: Caparica, Portugal, 2006.
23. NP EN450-1. *Cinzas Volantes Para Betão—Parte 1: Definição, Especificações e Critérios de Conformidade (Fly Ash for Concrete—Part 1: Definition, Specifications and Conformity Criteria)*; Instituto Português da Qualidade: Caparica, Portugal, 2012.
24. Granizo, M. Activation Alcalina de Metacaolin: Desarrollo de Nuevos Materiales Cementantes (Alkaline Metakaolin Activation: Development of New Binding Materials). Ph.D. Thesis, Universidad Autonoma de Madrid, Madrid, Germany, 1998; p. 325.
25. Granizo, M. Activation Alcalina de Metacaolin: Desarrollo de Nuevos Materiales Cementantes (Alkaline Metakaolin Activation: Development of New Binding Materials). PhD Thesis, Universidad Autonoma de Madrid, Madrid, Germany, 1998; p. 325.
26. Davidovits, J. Chemistry of Geopolymeric Systems, Terminology. In *Proceedings of 2nd International Conference Géopolymère*; Geopolymer Institute: Saint-Quentin, France, 1999; pp. 9–40.
27. Pinto, A. *Introdução ao Estudo dos Geopolímeros (Introduction to the Study of Geopolymers)*; Sector Editorial dos SDE-UTAD: Vila Real, Portugal, 2006; p. 79.
28. Neville, M. *Properties of Concrete*; John Wiley and Sons: New York, NY, USA, 1973.
29. NP EN196-1. *Métodos de Ensaio de Cimentos—Parte 1: Determinação das Resistências Mecânicas (Methods of Testing Cement. Determination of Strength)*; Instituto Português da Qualidade: Caparica, Portugal, 2006.
30. NP EN12390-5. *Ensaio do Betão Endurecido—Parte 5: Resistência à Flexão de Provetes (Testing Hardened Concrete. Flexural Strength of Test Specimens)*; Instituto Português da Qualidade: Caparica, Portugal, 2009.
31. NP EN 1998-1. 2009. *Eurocódigo 8: Projecto de Estruturas Para Resistência Aos Sismos. Parte 1: Regras Gerais, Acções Sísmicas e Regras Para Edifícios (Design of Structures for Earthquake Resistance. General Rules, Seismic Actions and Rules for Buildings)*; Instituto Português da Qualidade: Caparica, Portugal, 2010.

32. Lopes, A.V.; Lopes, S.M.R. Importance of a rigorous evaluation of the cracking moment in RC beams and slabs. *Comput. Concr.* **2012**, *9*, 275–291. [[CrossRef](#)]
33. Lopes, S.M.R.; Lopes, A.V.; Lou, T. Numerical Estimation of RC Beams. In Proceedings of the International Conference on Recent Advances in Nonlinear Models, Structural Concrete Applications, CoRAN 2011, Coimbra, Portugal, 24–25 November 2010; University of Coimbra: Coimbra, Portugal, 2011; pp. 243–253.
34. Lopes, A.V.; Lou, T.; Lopes, S.M.R. Nonlinear flexural behaviour of RC beams. In *Civil Engineering and the Concrete Future, Proceedings of the Twin Covilhã International Conferences, 5th Int'l Conference on the Concrete Future, Covilha, Portugal, 26–29 May 2013*; CI-Premier Pte Ltd.: Covilha, Portugal, 2013; pp. CF113–CF122.
35. NP EN 1992-1-1:2010. *Eurocódigo 2: Projeto de Estruturas de Betão; Parte 1: Regras Gerais e Regras Para Edifícios (Eurocode 2: Design of Concrete Structures. General Rules and Rules for Buildings)*; Instituto Português da Qualidade: Caparica, Portugal, 2010.
36. Lou, T.; Lopes, S.M.R.; Lopes, A.V. A finite element model to simulate long-term behavior of prestressed concrete girders. *Finite Elem. Anal. Des.* **2014**, *81*, 48–56. [[CrossRef](#)]



© 2020 by the authors. Licensee MDPI, Basel, Switzerland. This article is an open access article distributed under the terms and conditions of the Creative Commons Attribution (CC BY) license (<http://creativecommons.org/licenses/by/4.0/>).